Russian Chemical Bulletin, International Edition, Vol. 60, No. 8, pp. 1545—1555, August, 2011

Quantum chemical study of the charged gold atom influence on the mechanism of allylbenzene double bond migration

D. F. Mukhamedzyanova,[a]* D. A. Pichugina,[a,b] M. S. Askerka,[a] A. F. Shestakov,[b] and N. E. Kuz´menko[a]

[a]Department of Chemistry, M. V. Lomonosov Moscow State University,
1/3 Leninskie Gory, 119991 Moscow, Russian Federation.
Fax: +7 (495) 932 4765. E-mail: mukhamedzyanova@phys.chem.msu.ru
[b]Institute of Problems of Chemical Physics, Russian Academy of Sciences,
1 prosp. Akad. Semenova, 142432 Chernogolovka, Moscow Region, Russian Federation.
Fax: +7 (496) 515 5420. E-mail: a.s@icp.ac.ru

The DFT calculations of allylbenzene double bond migration were performed in the presence of gold ions Au^- and Au^+ and the cluster Au_4, which are models of active sites of the gold-containing catalysts. The mechanism of isomerization is determined by the charge of the metal. For the allylbenzene + Au^+ system, the most appropriate mechanism is the multistage metal-allylic process passing through either the formation of a gold-hydride complex, or no hydride complex is formed in the presence of Au^-. The calculated rate constant of the rate-determining step of the catalytic reaction increases in the order $Au^0 < Au^- < Au^+$. The $Au^{\delta+}$ particles are active sites in allylbenzene isomerization. Additional routes of accumulation of the *trans*-isomer result in the selective formation of *trans*-β-methylstyrene observed in the catalytic conversion of allylbenzene in the presence of gold nanoparticles. The metal-allylic mechanism is the most preferential in the presence of Au_4 cluster. The high energy of the bond of allylbenzene with the cluster is possibly due to the high reactivity of the latter.

Key words: DFT, PBE functional, double bond migration, mechanism of allylbenzene isomerization, gold clusters.

Isomerization of olefins is interesting from the viewpoint of fine organic synthesis and chemical technology. According to the Woodward—Hoffmann classification, hydrogen migration in hydrocarbon (1) is the [1,3]-sigmatropic shift.[1]

$$R{-}CH_2CH{=}CH_2 \longrightarrow R{-}CH{=}CHCH_3\ (\textit{trans} + \textit{cis}). \qquad (1)$$

Although the formation of the isomerization product is thermodynamically favorable in most cases, the reaction does not occur spontaneously because of high energy barriers.

Almost all compounds of *d*-elements catalyze double bond migration in olefins. Two main mechanisms of isomerization are distinguished, assuming the formation of metal-alkyl[2,3] or metal-allyl intermediates.[4,5] The isomerization of hex-1-ene to hex-2-ene on the palladium complexes includes alkene coordination to the Pd—H bond to form the π-complex and the further insertion of alkene into the Pd—H bond to form the σ-alkyl complex (metal-alkyl intermediate). β-Elimination of the reaction product occurs at the last stage.[6]

A similar mechanism was proposed for allylbenzene isomerization in the presence of the Ir^{III} complexes[7] and $HCo(CO)_4$.[8] In the presence of tungsten carbide,[9] but-1-ene is transformed into but-2-ene due to intramolecular hydrogen migration in the allylic system *via* two possible mechanisms to form various intermediates: metal-cyclobutane[10] or the π-allyl intermediate.[11] Double bond migration in terminal alkenes is catalyzed by the Pt^{II} complexes at relatively low temperatures.[12]

For allylbenzene isomerization, the ratio of *trans*/*cis* products achieves 98 : 2. The selectivity increases in favor of *trans*-β-methylstyrene due to the possibility of transformation of the Pt^{II}-*cis*-β-methylstyrene complex into the *trans*-product. The study of the mechanism of this reaction showed that the insertion of the substrate into the Pt—ligand bond at the intermediate stage resulted in the intermediate with the agostic Pt...H bond followed by β-hydride elimination.

Catalysts based on supported ultradispersed metal particles, including gold, become more and more popular in the recent time. They exhibit high activity and selectivity in many reactions involving hydrocarbons.[13—16] Allylbenzene ($PhCH_2CH{=}CH_2$) isomerization to *trans*- and *cis*-β-methylstyrene is catalyzed by gold nanoparticles supported on γ-Al_2O_3 (see Ref. 17). This reaction is interesting for investigation because of the size and synergetic

Published in Russian in *Izvestiya Akademii Nauk. Seriya Khimicheskaya,* No. 8, pp. 1521—1531, August, 2011.

effects found in the system. It was established, in particular, that metallic gold and large particles with the defect-free surface exhibit a substantially lower catalytic activity than the nanoparticles smaller than 40 nm.

The reaction rate increases, when nickel is introduced at the stage of metal particle growth, which is due to the coexistence of positively charged and neutral gold particles on the catalyst surface.[13] Another interesting feature of this reaction is associated with the selective formation of *trans*-β-methylstyrene, which is also characteristic, as it was shown, of the Pt^{II} complexes. For the metal particle size 13—34 nm, the *trans*/*cis* ratio was 4.7±0.2.[17] However, the nature of active sites, the reason for selective *trans*-β-methylstyrene formation, and the mechanism of allylbenzene isomerization in the presence of gold were not reliably determined.

One of the possible methods for studying the reaction mechanism is quantum chemical calculation, which makes it possible to predict the existence of the molecule and reveal the predominant direction of the chemical reaction. The catalytic properties of 1-ethyl-3-methylimidazolium towards the conversion of but-1-ene to but-2-ene were predicted[18] by the DFT methods (B3PW91/6-31G(d,p), 6-311++G(d,p), aug-cc-PVDZ). The assumed mechanism includes proton transfer from the imidazole ring to the terminal bond of hydrocarbon followed by the elimination of the proton from the adjacent ordinary bond.

It was shown[19] by the B3LYP/6-31G(d,p) method that the isomerization of pent-1-ene to pent-2-ene on the zeolite model can proceed *via* the step-by-step (E_a = = 31.5 kcal mol^{-1}) or concerted (E_a = 20.5 kcal mol^{-1}) mechanisms. In the first case, the reaction proceeds through the alkoxy intermediate. In the second case, the proton migration results in the formation of the final product pent-2-ene. The study of the isomerization of but-1-ene to but-2-ene by quantum chemical methods of various levels (DFT/PBE, MP2, CCSD) showed that even an isolated gold atom can be an efficient catalyst of the process that proceeds in several stages through the formation of the gold-hydride complex.[20]

According to numerous works[21—25] studying active sites of the gold-containing catalysts, surface atoms with maximum coordination unsaturation are the most active. Thus, it seems interesting to consider one gold atom represented the ultimate case of coordination unsaturation as the simplest model of the catalyst. The migration of the double bond of allylbenzene was studied in the presence of the neutral gold atom.[26] The reaction was found to proceed in four stages *via* the metal-allylic mechanism resulting in the migration of the hydrogen atom to the gold atom to form a gold-hydride complex. The high selectivity of *trans*-product formation was not explained for this model system.

It seems fruitful to compare the results obtained for the isolated atom with the data for the cluster containing more atoms. We chose the Au_4 cluster exhibiting a higher activity in the adsorption and activation of ethylene and hydrogen.[27—29] The study of the catalytic properties of molecular gold and silver clusters revealed their enhanced activity to CO oxidation, propene epoxidation, and propane dehydrogenation.[30] It was shown that the small clusters are catalytically more active than the large particles when they are simultaneously present on the metal surface.[31—33] The charge appeared on the active sites of the catalyst, for example, due to the interaction with the support or the synthesis method used[34—37] was simulated by the simplest Au^+ and Au^- ions.

In this work, we performed the quantum chemical simulation of allylbenzene isomerization to *cis*- and *trans*-β-methylstyrene on the gold ions and cluster and studied the influence of the gold atom charge on the mechanism and potential barriers. The study is aimed at determining the nature of active sites of the gold-containing catalysts in the migration of the double bond of allylbenzene, studying the mechanism of this reaction, and explaining the reason for the selective formation of *trans*-β-methylstyrene.

Calculation Procedure

The necessary calculations were performed using the Priroda 06 (see Ref. 38) and Gaussian 03 (see Ref. 39) programs in the framework of the DFT method with the PBE (Perdew—Burke—Ernzerhow) nonempirical functional.[40] Considerable relativistic effects for the gold atom were taken into account in the nonrelativistic approach using the SBK (Stevens—Basch—Krauss) pseudo-potential.[41] The following basis sets were used for the description of valent electrons: [311/1] for the H atom, [311/311/11] for four electrons of the C atom, and [51111/51111/5111] for 19 electrons of the Au atom.

Testing of the chosen method included a comparison of the calculated equilibrium interatomic distances (R_e) and dissociation energies (D_o or D_e) of molecules Au_2, AuH, and $AuCH_2^+$ with experimental values and hybrid B3LYP functional values (Table 1). It is seen that for the used basis set and pseudo-potential the PBE functional better describes the experimental data[42,43] than the B3LYP functional.

For the pseudo-potentials SBK, CEP-121G, LANL2DZ, and MWB60 using the PBE functional, the maximum deviations from the R_e values were 3, 7, 3, and 3% and those from the experimental values of D_o were 6, 4, 29, and 8%, respectively. Thus, the PBE/SBK method well describes the gold-containing systems.

It was shown[44,45] that the use of the SBK pseudo-potential in the DFT framework resulted in errors in equilibrium distances of ~0.001 Å for the systems consisting of the first-row elements (H) and 0.005—0.010 Å for the systems consisting of the second-row elements (C). The inaccuracy of the calculation of the relative energies is 10 kJ mol^{-1}. In this work, the interatomic distances are

Table 1. Calculated and experimental equilibrium interatomic distances (R_e/Å) and dissociation energies (D_o or D_e/eV) of molecules

Method	Au_2		AuH		$AuCH_2^+$	
	R_e	D_o	R_e	D_o	R_e (Au—C)	D_e
PBE/SBK	2.55	2.168	1.55	3.08	1.90	4.10
B3LYP/SBK	2.57	1.860	1.55	2.95	1.93	4.83
Experiment	2.472[42]	2.294[42]	1.5237[42]	3.209[42]	1.89[43]	>4.12[43]

given with the accuracy to 0.01 Å and the relative energies have the accuracy to 1 kJ mol^{-1}.

An additional testing calculation of some small gold-containing molecules was performed in the two-component scalar relativistic DFT approximation with the modified Dirac—Coulomb—Breit Hamiltonian.[46] A comparison of the values calculated in the nonrelativistic and scalar relativistic approaches revealed no especially preferred accuracy in any method. The nonrelativistic approach using the SBK pseudo-potential was applied to decrease time expenses to calculations.

The DFT calculations were carried out assuming that the reaction was adiabatic and the energy terms were not overlapped. This assumption is based on the data, according to which the ground electron states of the AuH ($^1\Sigma^+$) and Au_2 ($^1\Sigma_g{}^+$) molecules and Au_4 cluster ($^1A_1$) lie by 3.27 (see Ref. 47) and 2.277 (see Ref. 48) and by 0.98 eV (see Ref. 49) lower than the corresponding first excited states.

The relative energies were calculated including the zero-point vibration energies in the harmonic approximation. The bond energies (E_b) of a molecule of substrate **R** with the Au_n gold cluster were calculated using the formula

$$E_b = E^0(Au_n) + E^0(\mathbf{R}) - E^0(Au_n\mathbf{R}),$$

where $E^0(Au_n)$, $E^0(\mathbf{R})$, and $E^0(Au_n\mathbf{R})$ are the total energies including zero-point vibration energies of the isolated gold atom or cluster, the molecule and its complex with the atom or cluster, respectively.

The testing calculation of the error of the superposition of the basis set (BSSE) for some hydrocarbon complexes with gold atoms, ions, and clusters showed that the BSSE value changed from 0.3 to 2.3 kJ mol^{-1}, depending on the charge and size of the catalyst model. This correction is lower than the accuracy of the method used. The bond energies ignoring BSSE are presented. The atomic charges were calculated by a natural population analysis.

The study of the mechanism included the optimization procedure (search for local minima on the potential energy surface (PES)) for the geometries of the reactants (allylbenzene) and products (*cis*- and *trans*-β-methylstyrene) and their complexes with gold particles. The ground states with the spin multiplicity equal to 1 were studied for all systems. The structures of transition states were localized and identified, and the PES cross sections were constructed along the intrinsic reaction coordinates in the mass-weighted coordinates[50] by the Newton—Raphson method.[51] The type of stationary points on the PES was determined by analysis of the second derivative matrix. In some cases, scanning over the specified torsion angle was carried out.

The activation energy of each stage was calculated by the formula

$$E_a = E^0(\mathbf{TS}) - E^0(\mathbf{R}), \qquad (2)$$

where E_a is the activation energy, **TS** is the transition state, and **R** is the reactant. Based on the statistical sums of the starting substances, products, intermediates, and transition states, we determined the rate constants k of particular reaction stages using the activated complex theory[52] and the changes in the Gibbs energy ($\Delta_r G°$), enthalpy ($\Delta_r H°$), and entropy ($\Delta_r S°$) for these states at $T = 298$ K.

The energy diagrams were constructed for each possible reaction path. They represent the total energies of the reaction participants relative to the sum of energies of the isolated starting substances. One cycle is shown in each diagram: the process begins from the addition of allylbenzene to the gold atom and ceases by the desorption of β-methylstyrene with simultaneous binding of the next allylbenzene molecule with the gold particle.

Results and Discussion

Potential energy surface of the ground state of allylbenzene and β-methylstyrene

At the initial stage, the PES of the ground states of allylbenzene and products of its isomerization (*trans*- and *cis*-β-methylstyrenes) were studied and compared with the known values to check adequacy of the chosen method. Two conformers are known for $PhCH_2CH=CH_2$.[53—55] Scanning of the PES of allylbenzene over the C(1)C(2)—C(3)C(4) torsion angle (θ) confirmed the existence of stable conformational isomers **1a** (θ = 0°) and **1b** (θ = 123°) having close energies (Fig. 1).

The calculated interatomic distances and angles for the structures of allylbenzene conformers are consistent

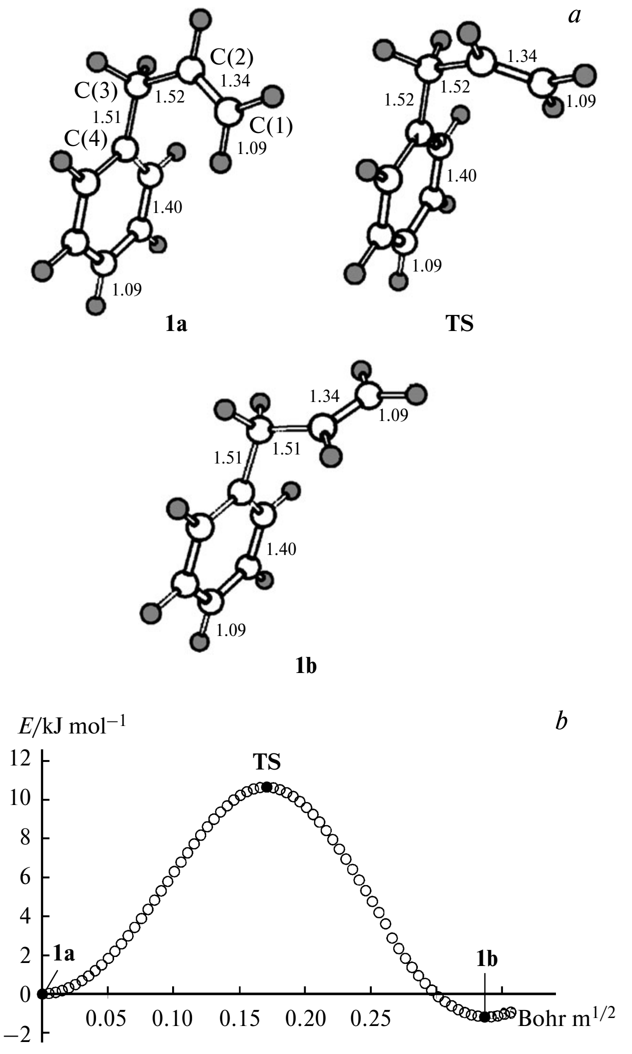

Fig. 1. Structures of stable conformers of allylbenzene **1a** and **1b** and transition state **TS** (*a*) and the PES cross section at the torsion angle C(1)C(2)C(3)C(4) of allylbenzene (*b*). The energy is given relative to conformer **1a**, and *s* is the internal coordinate of rotation relative to the torsion angle C(1)C(2)C(3)C(4). The calculated interatomic distances (Å) are presented.

with the published values.[55] The fundamental vibrations of hydrocarbon in the calculated IR spectrum well reproduce the experimentally known vibrational modes of allylbenzene.[56] The calculated rotation barrier about the C(2)—C(3) bond is 9 kJ mol^{-1}, which agrees with the data of the higher-level MP4(SDQ)/6-31G** method[55] (11 kJ mol^{-1}).

Thus, the chosen method satisfactorily describes the allylbenzene structure and qualitatively reproduces its vibrational modes and the difference in energies of two conformers. Due to free rotation, the existence of two conformers **1a** and **1b** are equiprobable. Designation **1** is accepted hereinafter for the both allylbenzene isomers.

Two structures were oprimized for β-methylstyrene: *cis*- and *trans*-configurations (**2a** and **2b**, respectively).

Table 2. Changes in the Gibbs energy $\Delta_r G°$ and enthalpy $\Delta_r H°$, the activation energy E_a, and the rate constant k for $PhCH_2CH=CH_2$ (**1**) isomerization to the *cis*- (**2a**) and *trans*-isomers (**2b**) of $PhCH=CHCH_3$

Reaction	Calculation				Experiment[56]
	$\Delta_r G°$	$\Delta_r H°$	E_a	k/s^{-1}	$\Delta_r H°$ /kJ mol^{-1}
	kJ mol^{-1}				
$\mathbf{1} \rightarrow \mathbf{TS_a} \rightarrow \mathbf{2a}$	−29	−16	234	$3 \cdot 10^{-29}$	−12.3±0.6
$\mathbf{1} \rightarrow \mathbf{TS_b} \rightarrow \mathbf{2b}$	−14	−28	234	$1 \cdot 10^{-29}$	−23.3±0.5

Torsion angle θ for isomer **2a** is 180°, and that for **2b** is 2°. *trans*-β-Methylstyrene is 11 kJ mol^{-1} more stable than the *cis*-isomer.

The simulation of double bond migration from position 1,2 of $PhCH_2CH=CH_2$ to position 2,3 showed that this process is thermodynamically favorable (Table 2). The calculated enthalpies of formation of *cis*- and *trans*-β-methylstyrene agree well with the experimental data.[56] The found transition state corresponds to the high activation energy for both *trans*- and *cis*-products. Therefore, this reaction does not occur spontaneously, and highly efficient catalysts capable of performing new routes with lower potential barriers are needed. According to the calculation, in the presence of the Au^0 gold atom, the activation energy of the rate-determining step of double bond migration in allylbenzene decreases.[26] Let us consider the systems with charged gold ions.

Migration of the double bond in allylbenzene in the presence of Au^- and Au^+ ions

System 1 + Au^-. The detailed study of allylbenzene isomerization in the presence of gold anions revealed three routes (Fig. 2). In the first case (route *1*), the reaction proceeds *via* the metal-allylic mechanism. At the first stage, $PhCH_2CH=CH_2$ is adsorbed to form complex $\mathbf{I}_1$ (E_b = 48 kJ mol^{-1}). Its structure differs strongly from a similar complex with the Au^0 atom,[26] which is remote at a considerable distance from the hydrocarbon, and the C=C bond is weakly activated. In the complex formed, the excessive negative charge partially shifted from the Au^- ion to the allylic system of the hydrocarbon. Then H^+ migrates from C(3) atom to the gold anion to form gold-hydride complex $\mathbf{I}_2$. The *trans*-β-methylstyrene—Au^- complex is formed through two intermediates ($\mathbf{I}_2$ and $\mathbf{I}_3$) with surmounting potential barriers of 82, 66, and 123 kJ mol^{-1}. In the *trans*-β-methylstyrene—Au^- complex, the gold particle is coordinated to none of the π-systems of the molecule.

The rate constant of the rate-determining step $\mathbf{I}_3 \rightarrow \mathbf{I}_4$ is $1 \cdot 10^{-9}$ s^{-1}, which is higher than that in the case of the Au^0 atom. The path of formation of *cis*-β-methylstyrene

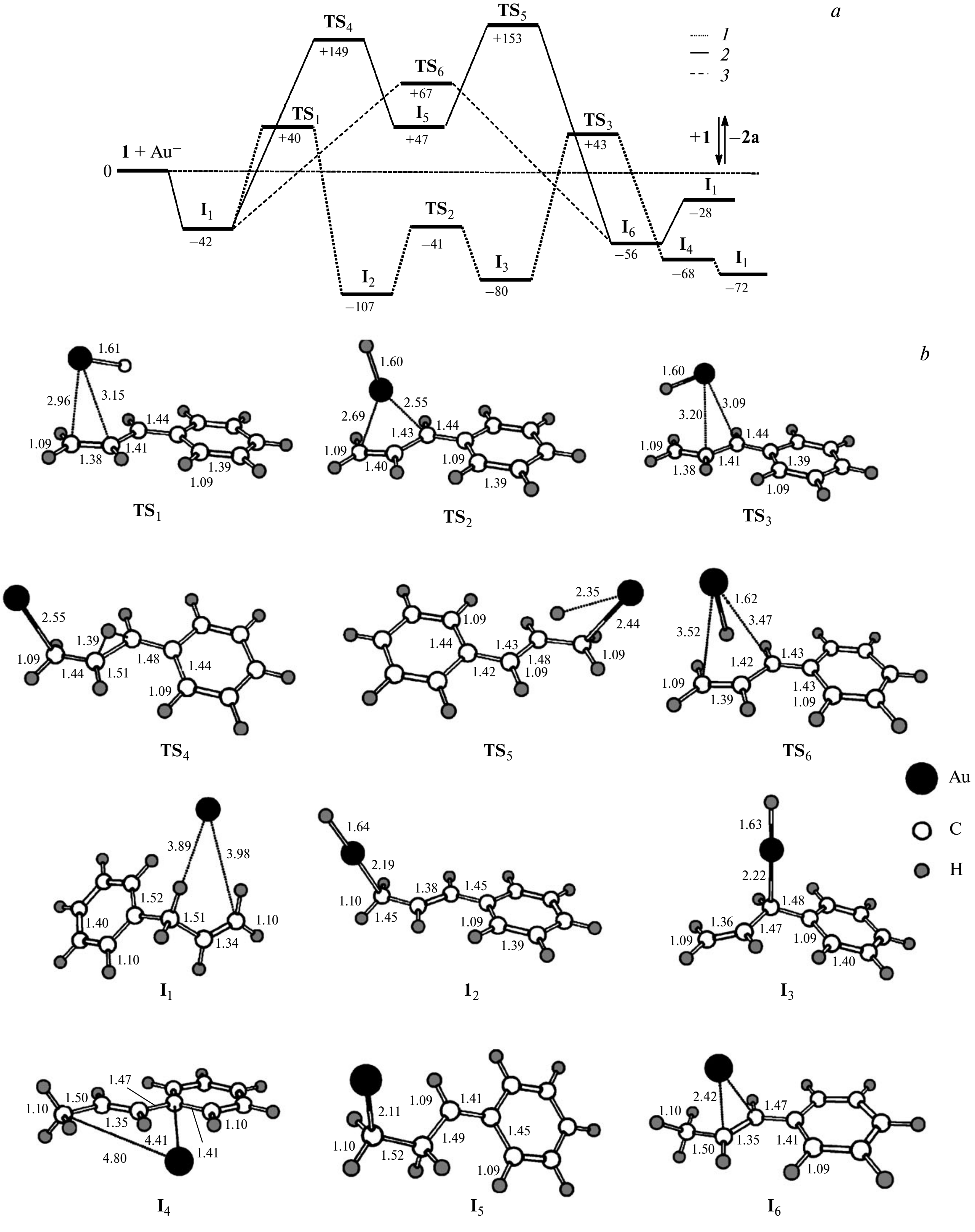

Fig. 2. Energy diagram of the formation of *trans*-β-methylstyrene in the system **1** + Au⁻ *via* routes (*1*), (*2*), and (*3*) (*a*) and the structures of transitions states and intermediates (*b*). The energies (E/kJ mol^{-1}) of the participants of the reaction are presented relative to the total energy of allylbenzene and Au⁻ (*a*), selected interatomic distances are indicated (Å) (*b*). Imaginary frequencies (ω_i) for the transition states, cm^{-1}: 381.90*i* (**TS**$_1$), 206.30*i* (**TS**$_2$), 399.00*i* (**TS**$_3$), 1170.20*i* (**TS**$_4$), 1159.80*i* (**TS**$_5$), and 853.90*i* (**TS**$_6$).

in the presence of the Au^- ion somewhat differs from the route found for the *trans*-isomer. The stage of formation of the gold-hydride complex occurs with a much higher potential barrier (97 kJ mol^{-1}) than a similar stage of *trans*-isomer formation. The difference by two orders of magnitude in the rate constants of the rate-determining step indicates the predominant formation of *trans*-β-methylstyrene.

In the second possible route (*2*), the proton does not shift to the gold atom but remains in the allylic system and transfers to the adjacent carbon atom (see Fig. 2). A similar mechanism was proposed[9] for but-1-ene isomerization to but-2-ene. *trans*-Product is formed through two transitions states $\mathbf{TS}_4$ and $\mathbf{TS}_5$ with activation energies of 191 and 106 kJ mol^{-1}, *i.e.*, higher than those for route (*1*). In this case, complex $\mathbf{I}_5$ is intermediate in which the migrating hydrogen atom is coordinated to the C(2) atom of the allylic system. The rate constant of the rate-determining step $\mathbf{I}_1 \to \mathbf{I}_5$ is $2 \cdot 10^{-22}$ s^{-1}, whereas that for the formation of the *cis*-product is $4 \cdot 10^{-25}$ s^{-1}.

The simplest is the third route (*3*) of double bond migration in the **1** + Au^- system.[11] In this case, the reaction does not involve the formation of the gold-hydride intermediate and the Au—H bond is formed only in the transition state (see Fig. 2). The allylbenzene—Au^- complex with E_b = 42 kJ mol^{-1} is transformed into the *trans*-β-methylstyrene—Au^- complex through one low potential barrier of 25 kJ mol^{-1}. The rate constant for the formation of *trans*-PhCH=CH—CH_3 is $2 \cdot 10^{-7}$ s^{-1}, which is two orders of magnitude higher than that for the formation of the *cis*-isomer. All kinetic and thermodynamic parameters calculated for the **1** + Au^- system are given in Table 3.

Thus, three directions of double bond migration are possible in the **1** + Au^- system (Scheme 1):

(*1*) metal-allylic mechanism, through the formation of the gold-hydride intermediate (four stages);

(*2*) allylic mechanism when H^+ remains in the allylic system and transfers to the adjacent carbon atom (four stages);

(*3*) allylic mechanism (three stages).

Table 3. Calculated changes in the Gibbs energy $\Delta_r G°$, enthalpy $\Delta_r H°$, and entropy of the reaction $\Delta_r S°$ (J mol^{-1} K^{-1}) and the rate constant *k* for allylbenzene isomerization to *trans*-β-methylstyrene in the presence of the Au^- ion

Stage	$\Delta_r G°$	$\Delta_r H°$	$\Delta_r S°$	k/s^{-1}
	kJ mol^{-1}		J mol^{-1} K^{-1}	
	Common stage for routes (*1*)—(*3*)			
1 + Au^- → $\mathbf{I}_1$	−188	−48	470	—
	(−182)	(−45)	(460)	—
	Route (*1*)			
$\mathbf{I}_1 \to \mathbf{I}_2$ ($\mathbf{TS}_1$)	−68	−77	−30	$2 \cdot 10^{-2}$
	(−60)	(−69)	(−30)	($6 \cdot 10^{-5}$)
$\mathbf{I}_2 \to \mathbf{I}_3$ ($\mathbf{TS}_2$)	23	25	9	18
	(22)	(23)	(2)	(32)
$\mathbf{I}_3 \to \mathbf{I}_4$ ($\mathbf{TS}_3$)	18	−91	32	$1 \cdot 10^{-9}$
	(22)	(27)	(18)	($4 \cdot 10^{-11}$)
$\mathbf{I}_4$ → **2a** + Au^-	182	42	−471	—
	(184)	(−48)	(456)	—
	Route (*2*)			
$\mathbf{I}_1 \to \mathbf{I}_5$ ($\mathbf{TS}_4$)	94	88	−20	$2 \cdot 10^{-22}$
	(49)	(41)	(−27)	($4 \cdot 10^{-25}$)
$\mathbf{I}_5 \to \mathbf{I}_6$ ($\mathbf{TS}_5$)	−102	−102	−1	$2 \cdot 10^{-6}$
	(−45)	(−43)	(7)	($1 \cdot 10^{-15}$)
$\mathbf{I}_6$ → **2a** + Au^-	195	33	−543	—
	(164)	(32)	(−443)	—
	Route (*3*)			
$\mathbf{I}_1 \to \mathbf{I}_6$ ($\mathbf{TS}_6$)	−9	−16	−24	$2 \cdot 10^{-7}$
	(5)	(−1)	(−20)	($6 \cdot 10^{-9}$)
$\mathbf{I}_6$ → **2a** + Au^-	164	33	437	—
	(196)	(28)	(561)	—

Note. Temperature 298 K. The designations of the reactants in the stages are presented in Fig. 2. The values for the formation of the *cis*-isomer are given in parentheses.

Route (*3*) is most preferable from the kinetic point of view. Substantial difference between the rate constants of formation of the *trans*- and *cis*-isomers were found for the **1** + Au^- system and were not observed in the case of the Au^0 atom.

System 1 + Au^+. Routes (*1*) and (*2*) were studied for the **1** + Au^+ system, but the transition state of route (*3*) was not localized (see Scheme 1). At the first stage, the allylbenzene—Au^+ prereaction complex is formed with

Scheme 1

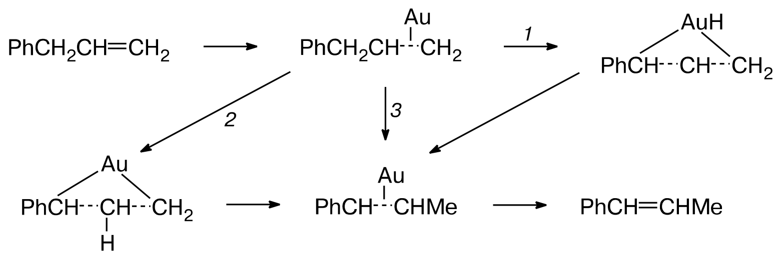

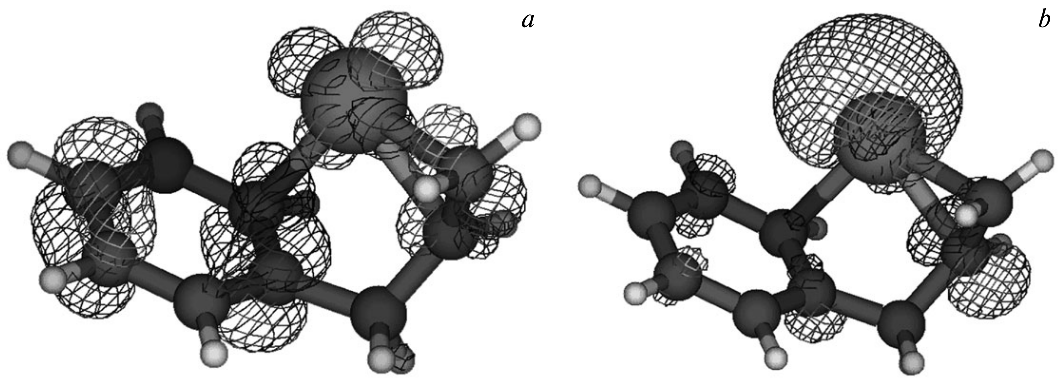

Fig. 3. Visualization of the frontier molecular orbitals of the most stable (in energy) allylbenzene—Au$^+$ complex: HOMO (*a*) and LUMO (*b*).

a significant energy gain and forming the strong bond between the electron-deficient gold ion and the π-system of the double bond of allylbenzene and/or benzene ring. This is due to the fact that the lowest unoccupied molecular orbital (LUMO) of the positively charged gold ion is closer by energy to the highest occupied molecular orbital (HOMO) of the olefin, facilitating the electron density transfer from the HOMO of allylbenzene to the LUMO of the gold ion and the backward process. A substantial feature of the bond between the gold particle and the unsaturated hydrocarbon system is the interaction between the π-orbital of allylbenzene (HOMO$_{\text{alkene}}$) and the vacant *s*-orbital of the Au$^+$ ion (LUMO$_{\text{Au+}}$), resulting in the electron density transfer from the alkene to the metal. However, there is a compensating flow caused by the overlapping of the occupied *d*-orbital (HOMO$_{\text{Au+}}$) of the gold ion with the vacant antibonding π-orbital (LUMO$_{\text{alkene}}$) of allylbenzene (Fig. 3).

A similar qualitative structure of the molecular orbitals for the formation of the metal—ethylene bond has been proposed earlier.[57] No efficient overlapping of the molecular orbitals of the gold particles and hydrocarbon upon the formation of the prereaction complex was observed for the previous systems.

In the presence of the Au$^+$ ion, *trans*-β-methylstyrene is formed through two gold-hydride intermediates **I**$_8$ and **I**$_9$ with different coordination of the gold particle to the allylic system (Figs 4 and 5). In complex **I**$_8$, coordination with the gold particle involves the C(4) and C(3) atoms of the benzene ring. In intermediate **I**$_9$, binding occurs at the C(1) and C(2) terminal atoms. Two paths of *trans*-isomer formation become possible due to the existence of two gold-hydride intermediates in the **1** + Au$^+$ system (see Figs 4 and 5).

The first path **I**$_7$ → **2a** passes through intermediate **I**$_8$. The rate constant of the rate-determining step of the first path (**I**$_8$ → **I**$_{11}$) is $4 \cdot 10^{-6}$ s^{-1}. The second path **I**$_7$ → **2a** passes through intermediates **I**$_8$ and **I**$_9$, and the potential barriers of the latter two stages decrease. The rate constant of the rate-determining step of isomerization *via* the sec-

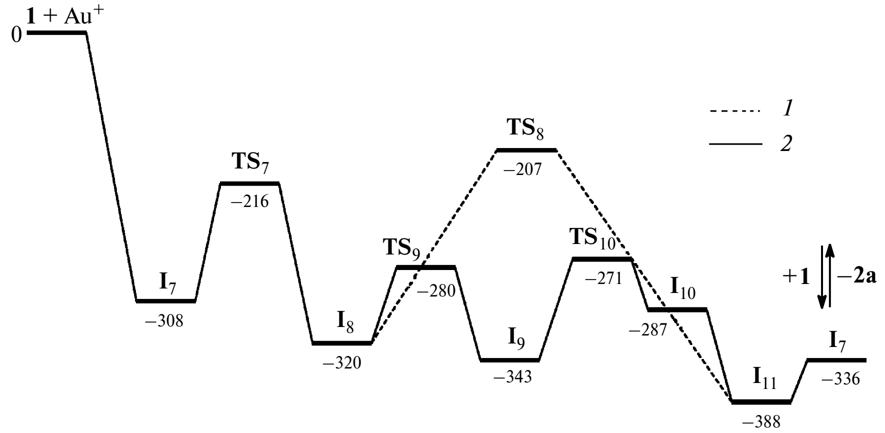

Fig. 4. Energy diagram of the formation of *trans*-β-methylstyrene in the **1** + Au$^+$ system *via* route (*1*) with paths *1* and *2*. The energies (E/kJ mol^{-1}) of the participants of the reaction are presented relative to the total energy of allylbenzene and Au$^+$. Imaginary frequencies (ω_i) for the transition states, cm^{-1}: 131.40*i* (**TS**$_7$), 674.20*i* (**TS**$_8$), 96.10*i* (**TS**$_9$), and 226.60*i* (**TS**$_{10}$).

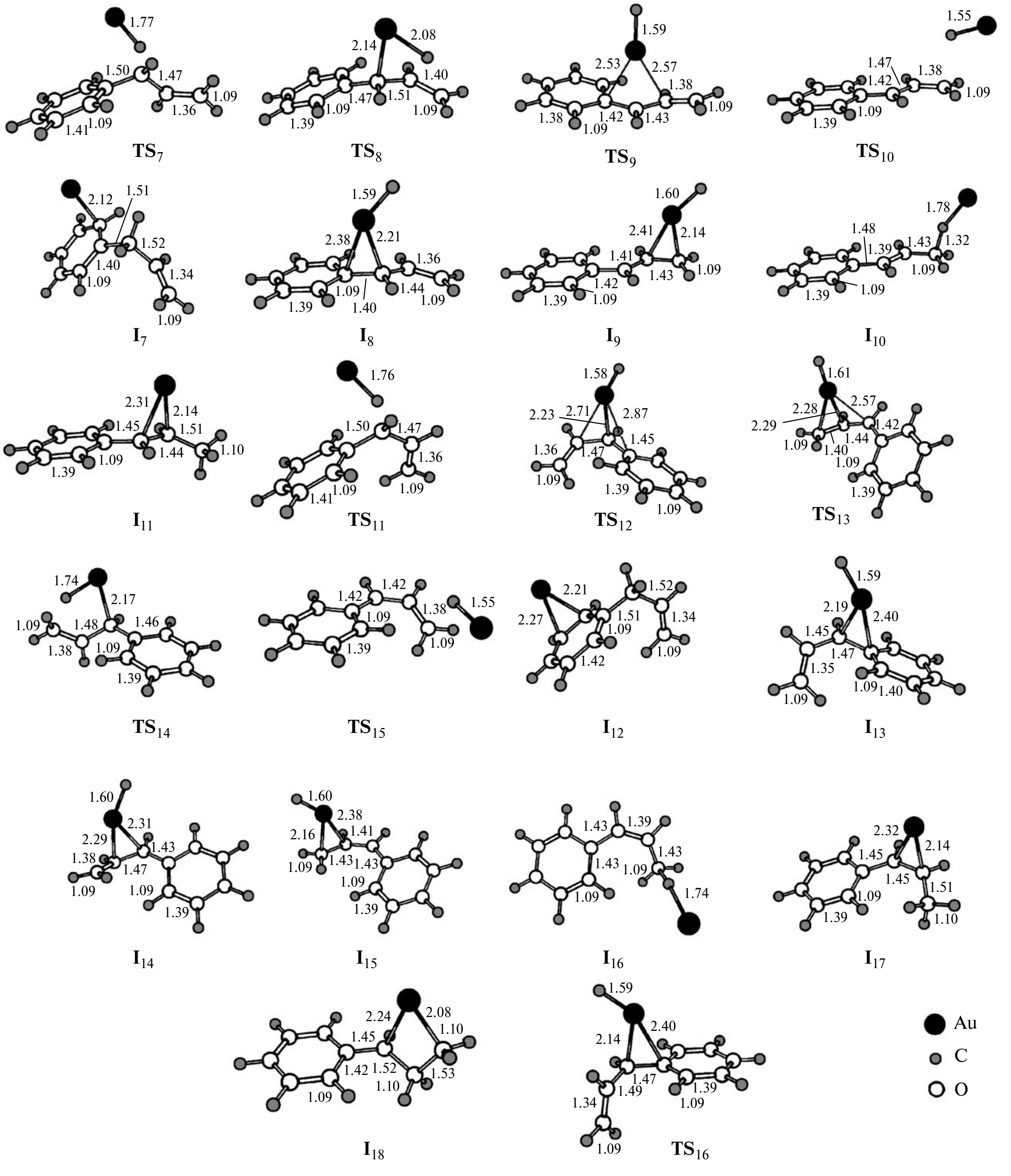

Fig. 5. Structures of the transition states and intermediates presented in Figs 4 and 6, intermediate $\mathbf{I}_{18}$ in the formation of the *trans*-isomer in the **1** + Au^+ system *via* route (*2*), and transition state $\mathbf{TS}_{16}$ of the stage of the rotation about C(2)—C(3) bond in gold-hydride complex. Selected interatomic distances (Å) are presented.

ond path ($\mathbf{I}_7 \to \mathbf{I}_8$) is $9 \cdot 10^{-5}$ s^{-1}. The H^- hydride ion migrates to the gold particle. Regardless of the choice of the first or second path, the less stable complex *trans*-β-methylstyrene—Au^+ ($\mathbf{I}_{10}$) is formed at the final stage and is isomerized to a more stable complex $\mathbf{I}_{11}$ with an energy gain of 101 kJ mol^{-1}. *trans*-β-Methylstyrene is desorbed from intermediate $\mathbf{I}_{10}$ or $\mathbf{I}_{11}$, and the latter process requires 360 kJ mol^{-1} to occur. A comparison of the constants of the rate-determining steps of the formation *via* the first or second path shows that the transformation into

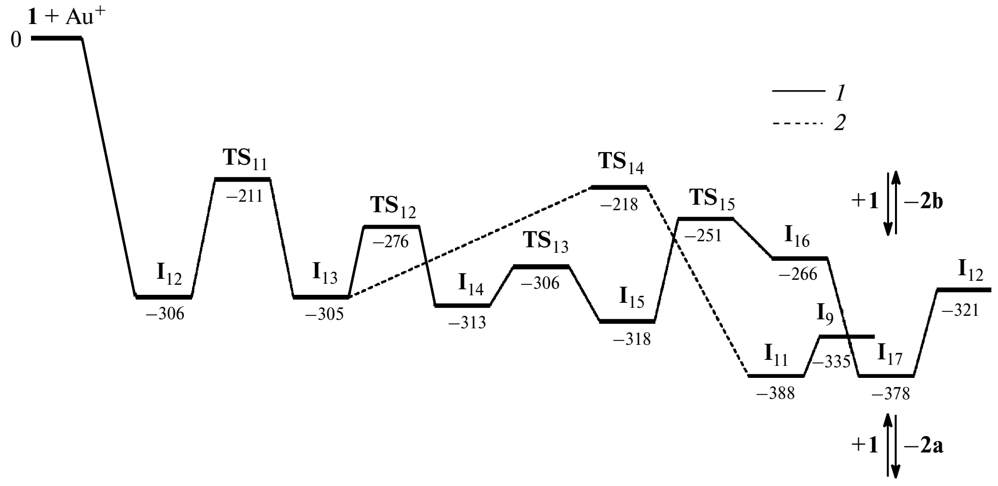

Fig. 6. Energy diagram of the formation of *cis*-β-methylstyrene (*1*) and *trans*-β-methylstyrene (*2*) in the **1** + Au$^+$ system *via* route (*1*). The energies (E/kJ mol^{-1}) of the participants of the reaction are presented relative to the total energy of allylbenzene and Au$^+$. Imaginary frequencies (ω_i) for the transition states, cm^{-1}: 139.10*i* ($\mathbf{TS}_{11}$), 96.10*i* ($\mathbf{TS}_{12}$), 319.80*i* ($\mathbf{TS}_{13}$), 232.20*i* ($\mathbf{TS}_{14}$), and 731.60*i* ($\mathbf{TS}_{15}$).

trans-β-methylstyrene through intermediates $\mathbf{I}_8$ and $\mathbf{I}_9$ is the most favorable.

A more complicated path *via* the metal-allylic mechanism through three gold-hydride complexes ($\mathbf{I}_{13}$, $\mathbf{I}_{14}$, and $\mathbf{I}_{15}$) differed by the position of the Au—H fragment in the allylic system (see Figs 5 and 6) was found for the formation of *cis*-β-methylstyrene. The rate constant of the rate-determining step of isomerization ($\mathbf{I}_{12} \rightarrow \mathbf{I}_{13}$) is $6 \cdot 10^{-5}$ s^{-1}. It should be mentioned that an alternative transformation of gold-hydride complex $\mathbf{I}_{13}$ is possible not into $\mathbf{I}_{14}$ and further into the *cis*-isomer, but into the *trans*-β-methylstyrene—Au$^+$ complex ($\mathbf{I}_{11}$) through a potential barrier of 87 kJ mol^{-1}. The stage of formation of intermediate $\mathbf{I}_{13}$ is the same in two routes (see Fig. 6) and, hence, the both directions are equiprobable and competing. Thus, an additional path for *trans*-isomer formation was found.

An alternative route (*2*) was studied for the **1** + Au$^+$ system (see Scheme 1). Let us consider the results obtained for the formation of *trans*-β-methylstyrene, since similar regularities are observed for the *cis*-product. For the mechanism studied, the intermediate differs strongly from complexes $\mathbf{I}_8$ and $\mathbf{I}_9$ by the coordination of the hydride ion. The activation energy of intermediate formation is 84 kJ mol^{-1}. Complex $\mathbf{I}_{18}$ is formed at the intermediate state (see Fig. 5), and its structure is similar to metal—cycloalkane.[10] Path (*2*) is less probable, because the rate constant for the rate-determining step is two orders of magnitude lower than that for the slowest stage of route (*1*). The thermodynamic and kinetic parameters of the studied routes of the isomerization reaction in the **1** + Au$^+$ system are listed in Table 4.

Thus, the double bond migration can occur *via* several routes depending on the charge of the active site. According to the calculation, the metal-allylic mechanism is pref-

Table 4. Calculated changes in the Gibbs energy $\Delta_r G°$, enthalpy $\Delta_r H°$, and entropy of the reaction $\Delta_r S°$ (J mol^{-1} K^{-1}) and the rate constant k for allylbenzene isomerization in the presence of the Au$^+$ ion

Stage	$\Delta_r G°$	$\Delta_r H°$	$\Delta_r S°$	k/s^{-1}
	kJ mol^{-1}		J mol^{-1} K^{-1}	
Allylbenzene + Au$^+$ = *trans*-β-methylstyrene + Au$^+$ Common stages for paths (*1*) and (*2*)				
1 + Au$^+$ → $\mathbf{I}_7$	−445	−310	453	—
$\mathbf{I}_7$ → $\mathbf{I}_8$ ($\mathbf{TS}_7$)	−16	−20	−13	$8 \cdot 10^{-5}$
Path (*1*)				
$\mathbf{I}_8$ → $\mathbf{I}_{11}$ ($\mathbf{TS}_8$)	−56	−59	−8	$4 \cdot 10^{-6}$
$\mathbf{I}_{11}$ → **2a** + Au$^+$	484	358	−423	—
Path (*2*)				
$\mathbf{I}_8$ → $\mathbf{I}_9$ ($\mathbf{TS}_9$)	−22	−23	−3	$3 \cdot 10^{5}$
$\mathbf{I}_9$ → $\mathbf{I}_{10}$ ($\mathbf{TS}_{10}$)	51	55	13	$3 \cdot 10^{2}$
$\mathbf{I}_{10}$ → $\mathbf{I}_{11}$	−85	−91	−18	—
$\mathbf{I}_{11}$ → **2a** + Au$^+$	484	358	−423	—
Allylbenzene + Au$^+$ = *cis*-β-methylstyrene + Au$^+$				
I + Au$^+$ → $\mathbf{I}_{12}$	−436	−306	−195	—
$\mathbf{I}_{12}$ → $\mathbf{I}_{13}$ ($\mathbf{TS}_{11}$)	−5	−8	−10	$5 \cdot 10^{-5}$
$\mathbf{I}_{13}$ → $\mathbf{I}_{14}$ ($\mathbf{TS}_{12}$)	−4	−6	−7	$3 \cdot 10^{7}$
$\mathbf{I}_{14}$ → $\mathbf{I}_{15}$ ($\mathbf{TS}_{13}$)	−8	−8	11	$4 \cdot 10^{11}$
$\mathbf{I}_{15}$ → $\mathbf{I}_{16}$ ($\mathbf{TS}_{15}$)	48	51	9	$2 \cdot 10^{-2}$
$\mathbf{I}_{16}$ → $\mathbf{I}_{17}$	−97	−101	−15	—
$\mathbf{I}_{17}$ → **2b** + Au$^+$	488	360	−430	—
$\mathbf{I}_{13}$ → $\mathbf{I}_{11}$ ($\mathbf{TS}_{14}$)*	−71	−72	−3	$2 \cdot 10^{-5}$
$\mathbf{I}_{11}$ → **2a** + Au^{+}*	484	358	−423	—

* Additional path for the formation of *trans*-β-methylstyrene. Temperature 298 K. The designations of the reactants in the stages are given in Figs 4—6.

erable for the **1** + Au^+ system, whereas the path without intermediate formation is preferable for the **1** + Au^- system. The bond energy of allylbenzene with the gold particle increases on going from the negatively charged ion to the positive one

$$Au^- (42\ kJ\ mol^{-1}) < Au^0 (59\ kJ\ mol^{-1}) << Au^+ (308\ kJ\ mol^{-1}).$$

The activation energy of the rate-determining stage of the optimum path of *trans*-isomer formation increases on going from the charged ions to the neutral gold atom

$$Au^+ (92\ kJ\ mol^{-1}) < Au^- (109\ kJ\ mol^{-1}) < Au^0 (146\ kJ\ mol^{-1}).$$

According to the calculations, the $Au^{\delta+}$ sites are active in the isomerization of allylbenzene.

Selective formation of *trans*-β-methylstyrene in the 1 + Au^+ system used as an example

As mentioned above, double bond migration in allylbenzene is characterized by the selective formation of *trans*-β-methylstyrene. When studying the migration of the double bond, we found an additional path for *trans*-isomer formation competing with the route of formation of the *cis*-product.

In order to understand in detail selectivity for allylbenzene isomerization in the presence of the Au^+ ion, we used the assumption about the possibility of rotation about the C(2)—C(3) bond in gold-hydride complex $\mathbf{I}_{13}$. Transition state $\mathbf{TS}_{16}$ (see Fig. 5) corresponding to transformation $\mathbf{I}_{13} \to \mathbf{I}_8$ was found by scanning of the PES of complex $\mathbf{I}_{13}$ over the C(1)C(2)C(3)C(4) torsion angle. The energy barrier of this transformation is rather low: 27 kJ mol^{-1}. Therefore, the two routes of formation of the *cis*- and *trans*-isomers can intersect, which will lead to the predominant formation of *trans*-β-methylstyrene.

The mechanism *via* the gold-hydride intermediate is preferable for the **1** + Au^+ system. The additional routes found for the formation of the *trans*-product indicate its predominant accumulation over the *cis*-isomer.

Double bond migration in allylbenzene in the presence of the Au_4 cluster

Neutral cluster Au_4 was chosen as a model of the active site of the gold-containing catalyst to estimate the influence of the cluster composition on the reaction mechanism and potential barriers. The mechanism of allylbenzene isomerization was chosen using the formation of *cis*-β-methylstyrene as an example. Two mechanisms similar to those described above (routes (*1*) and (*2*), see Scheme 1) were found for the **1** + Au_4 system.

The first stage of the metal-allylic mechanism is the formation of the allylbenzene—Au_4 complex with an energy gain of 138 kJ mol^{-1}, which considerably exceeds[26] that for the **1** + Au^0 system — 51 kJ mol^{-1}. A similar adsorption activity of the Au_4 cluster is observed for ethylene adsorption[28]: the heat of adsorption on the Au_4 cluster is 139 kJ mol^{-1}, whereas that on one gold atom is 46 kJ mol^{-1}. A significant activation of the olefin occurs upon the formation of the allylbenzene—Au_4 complex, because the elongation of the C=C bond reaches 1.40 Å. At the next stage, H^+ migrates to form an intermediate over a potential barrier of 136 kJ mol^{-1}, which is comparable with the activation energy at the second stage of *cis*-isomer formation in the **1** + Au^0 system (E_a = 134 kJ mol^{-1}). The electron density of the allylic system in the intermediate is concentrated between the C(2) and C(3) atoms, indicating double bond migration already at the stage of hydride complex formation. The rate constant of the rate-determining stage of gold-hydride complex formation is $5 \cdot 10^{-11}$ s^{-1}.

According to the results obtained, with an increase in the number of gold atoms in the cluster, the values of potential barriers and the reaction mechanism remain almost unchanged compared to those for one gold atom.

***

The study of allylbenzene isomerization showed that the double bond migration can occur *via* three directions, among which the metal-allylic mechanism is preferable for the allylbenzene + Au^+ system and the path without gold-hydride intermediate formation is preferable for the allylbenzene + Au^- system. An increase in the size of the gold cluster to Au_4 does not substantially change the regularities obtained earlier for the mechanism of double bond migration in allylbenzene in the presence of the Au^0 neutral atom.

In the allylbenzene + Au^+ system, the transition states found correspond to the lower activation energies than those for the neutral and negatively charged gold particles. Thus, according to the calculation data, the $Au^{\delta+}$ ions are active sites in allylbenzene isomerization. The reason for the selective formation of *trans*-β-methylstyrene observed for the catalytic conversion of allylbenzene in the presence of gold nanoparticles is the presence of additional routes of *trans*-isomer accumulation with the lower potential barriers compared to the formation of the *cis*-isomer.

This work was financially supported by the Russian Foundation for Basic Research (Project No. 10.03.00999) and the Council on Grants at the President of the Russian Federation (Program for State Support of Leading Scientific Schools of the Russian Federation, Grant NSh 6512.2010.3).

References

1. O. A. Reutov, A. L. Kurts, K. P Butin, *Organicheskaya khimiya* [*Organic Chemistry*], **4**, Izd-vo MGU, Moscow, 1999, 340 (in Russian).

2. C. Masters, *Homogeneous transition-metal catalysis*, Chapman and Hall, New York, 1977, 277 pp.
3. K. J. Klabunde, Y. Tanaka, *J. Mol. Catal.*, 1983, **21**, 57.
4. Z. Wu, C. Li, P. Ying, Z. Wei, Q. Xin, *J. Phys. Chem.*, 2001, **105**, 9183.
5. J. C. Sworen, J. H. Pawlow, W. Case, J. Lever, K. B. Wagener, *J. Mol. Catal.*, 2003, **194**, 69.
6. G. Myagmarsuren, V. S. Tkach, F. K. Shmidt, *React. Kinet. Catal. Lett.*, 2004, **83**, 337.
7. A. C. Cooper, K. G. Caulton, *Inorg. Chim. Act.*, 1996, **251**, 41.
8. R. F. Heck, D. S. Breslow, *J. Am. Chem. Soc.*, 1961, **83**, 4023.
9. V. Keller, R. Touroude, G. Maire, *Catal. Lett.*, 1997, **47**, 63.
10. J. J. Rooney, G. Webb, *J. Catal.*, 1964, **3**, 488.
11. J. Goetz, M. A. Volpe, R. Touroude, *J. Catal.*, 1996, **164**, 369.
12. A. Scarso, M. Colladon, P. Sgarbossa, C. Santo, R. A. Michelin, G. Strukul, *Organometallics*, 2010, **29**, 1487.
13. O. P. Tkachenko, L. M. Kustov, S. A. Nikolaev, V. V. Smirnov, K. V. Klementiev, A. V. Naumkin, I. O. Volkov, A. Yu. Vasil´kov, D. Yu. Murzine, *Top. Catal.*, 2009, **52**, 344.
14. T. Hayashi, K. Tanaka, M. Haruta, *J. Catal.*, 1998, **178**, 566.
15. C. Mohr, H. Hofmeister, J. Radnik, P. Claus, *J. Am. Chem. Soc.*, 2003, **125**, 1905.
16. S. A. Nikolaev, V. V. Smirnov, *Gold. Bull.*, 2009, **42**, 182.
17. V. V. Smirnov, S. A. Nikolaev, G. P. Murav´eva, L. A. Tyurina, A. Yu. Vasil´kov, *Kinet. Katal.*, 2007, **48**, 281 [*Kinet. Catal.* (*Engl. Transl.*), 2007, **48**, 265].
18. M. Pu, B.-H. Chen, H.-X. Wang, *Chem. Phys. Lett.*, 2005, **410**, 441.
19. Y.-H. Guo, M. Pu, L.-Y. Liu, H.-F. Li, B.-H. Chen, *Comput. Mater. Sci.*, 2008, **42**, 179.
20. D. A. Pichugina, A. F. Shestakov, N. E. Kuz´menko, *Izv. Akad. Nauk*, *Ser. Khim.*, 2008, 1330 [*Russ. Chem. Bull., Int. Ed.*, 2008, **57**, 1356].
21. J. D. Grunwaldt, M. Maciejewski, O. S. Becker, P. Fabrizioli, A. Baiker, *J. Catal.*, 1999, **186**, 458.
22. N. Lopez, J. K. Nørskov, *Surf. Sci.*, 2002, **515**, 175.
23. X. Deng, B. K. Min, A. Guloy, C. M. Friend, *J. Am. Chem. Soc.*, 2005, **127**, 9267.
24. T. V. W. Janssens, A. Carlsson, A. Puig-Molina, B. S. Clausen, *J. Catal.*, 2006, **240**, 108.
25. T. V. W. Janssens, B. S. Clausen, B. Hvolbek, H. Falsig, C. H. Christensen, T. Bligaard, J. K. Nørskov, *Top. Cat.*, 2007, **44**, 15.
26. D. A. Pichugina, S. A. Nikolaev, D. F. Mukhamedzyanova, A. F. Shestakov, N. E. Kuz´menko, *Zh. Fiz. Khim.*, 2011, **85**, 724 [*Russ. J. Phys. Chem.* (*Engl. Transl.*), 2011, **85**].
27. G.-J. Kang, Z.-X. Chen, Z. Li, *J. Chem. Phys.*, 2009, **131**, 034710.
28. A. Lyalin, T. Taketsuga, *J. Chem. Phys.*, 2010, **114**, 2484.
29. G.-J. Kang, Z.-X. Chen, Z. Li, X. He, *J. Chem Phys.*, 2009, **130**, 034701.
30. S. Chrétien, S. K. Buratto, H. Metiu, *Current Opinion in Solid State and Materials Science*, 2007, **11**, 62.
31. Q. Fu, H. Saltsburg, M. Flytzani-Stephanopoulos, *Science*, 2003, **301**, 935.
32. W. E. Kadden, T. Wu, W. A. Kunkel, S. L. Anderson, *Science*, 2009, **326**, 826.
33. A. A. Herzing, C. J. Kiely, A. F. Carley, P. Landon, G. J. Hutchings, *Science*, 2008, **321**, 1331.
34. A. Sanchez, S. Abbet, U. Heiz, W.-D. Schneider, H. Häkkinen, R. N. Barnett, U. Landman, *J. Phys. Chem. A.*, 1999, **103**, 9573.
35. D. Ricci, A. Bongiorno, G. Pacchioni, U. Landman, *Phys. Rev. Lett.*, 2006, **97**, 036106.
36. M. Chen, D. W. Goodman, *Chem. Soc. Rev.*, 2008, **37**, 1860.
37. W. T. Wallace, B. K. Min, D. W. Goodman, *Top. Cat.*, 2005, **34**, 17.
38. Yu. A. Ustynyuk, D. N. Laikov, *Izv. Akad. Nauk*, *Ser. Khim.*, 2005, 804 [*Russ. Chem. Bull., Int. Ed.*, 2005, **54**, 820].
39. M. J. Frisch, G. W. Trucks, H. B. Schlegel, G. E. Scuseria, M. A. Robb, J. R. Cheeseman, J. A. Montgomery, Jr. T. Vreven, K. N. Kudin, J. C. Burant, J. M. Millam, S. S. Iyengar, J. Tomasi, V. Barone, B. Mennucci, M. Cossi, G. Scalmani, N. Rega, G. A. Petersson, H. Nakatsuji, M. Hada, M. Ehara, K. Toyota, R. Fukuda, J. Hasegawa, M. Ishida, T. Nakajima, Y. Honda, O. Kitao, H. Nakai, M. Klene, X. Li, J. E. Knox, H. P. Hratchian, J. B. Cross, C. Adamo, J. Jaramillo, R. Gomperts, R. E. Stratmann, O. Yazyev, A. J. Austin, R. Cammi, C. Pomelli, J. W. Ochterski, P. Y. Ayala, K. Morokuma, G. A. Voth, P. Salvador, J. J. Dannenberg, V. G. Zakrzewski, S. Dapprich, A.D. Daniels, M. C. Strain, O. Farkas, D. K. Malick, A. D. Rabuck, K. Raghavachari, J. B. Foresman, J. V. Ortiz, Q. Cui, A. G. Baboul, S. Clifford, J. Cioslowski, B. B. Stefanov, G. Liu, A. Liashenko, P. Piskorz, I. Komaromi, R. L. Martin, D.J. Fox, T. Keith, M. A. Al-Laham, C. Y. Peng, A. Nanayakkara, M. Challacombe, P. M. W. Gill, B. Johnson, W. Chen, M. W. Wong, C. Gonzalez, J. A. Pople, *Gaussian 03, Revision A.1*, Gaussian Inc., Pittsburgh PA, 2003.
40. J. P. Perdew, K. Burke, M. Ernzerhoff, *Phys. Rev. Lett.*, 1996, **77**, 3865.
41. W. J. Stevens, M. Krauss, *J. Chem.*, 1992, **70**, 612.
42. K. S. Krasnov, *Molekulyarnye postoyannye neorganicheskikh soedinenii* [*Molecular Constants of Inorganic Compounds*], Khimiya, Leningrad, 1979, 445 (in Russian).
43. A. K. Chowdhury, C. L. Wilkins, *J. Am. Chem. Soc.*, 1987, **109**, 5336.
44. C. Janfelt, F. Jensen, *Chem. Phys. Lett.*, 2005, **406**, 501.
45. F. Jensen, C. Janfelt, *Chem. Phys. Lett.*, 2005, **412**, 12.
46. K. G. Dyall, *J. Chem. Phys.*, 1994, **100**, 2118.
47. H. A. Witek, T. Nakijima, K. Hirao, *J. Chem. Phys.*, 2000, **113**, 8015.
48. I. Itkin, A. Zaitsevskii, *Chem. Phys. Lett.*, 2003, **374**, 143.
49. K. Balasubramanian, P. Y. Feng, M. Z. Liao, *J. Chem. Phys.*, 1989, **91**, 3561.
50. C. Gonzalez, H. B. Schlegel, *J. Chem. Phys.*, 1989, **90**, 2154.
51. E. S. Apostolova, A. I. Mikhailyuk, V. G. Tsirel´son, *Kvantovo-khimicheskoe opisanie reaktsii* [*Quantum Chemical Description of Reactions*], RKhTU, Moscow, 1999, 61 (in Russian).
52. S. Glasstone, K. J. Laidler, H. Eyring, *The Theory of Rate Processes*, McGraw-Hill Book, New York, 1941, 611 pp.
53. C. Kolczewski, F. J. Williams, R. L. Cropley, *J. Chem. Phys.*, 2006, **125**, 034701.
54. P. J. Breen, E. R. Bernstein, *J. Phys. Chem.*, 1989, **93**, 6731.
55. J. Urban, P. Mach, J. Leszczynski, *Struct. Chem.*, 1999, **10**, 79.
56. *NIST Standard Reference Database 69*, 2005.
57. J. N. Murrell, S. F. Kettle, J. M. Tedder, *The Chemical Bond*, John Wiley and Sons, Inc., New York, 1978, 333 pp.

Received December 24, 2010;
in revised form May 11, 2011